A multimodal nonlinear piezoelectric vibration absorber

G. Raze[1], **B. Lossouarn**[2], **A. Paknejad**[3], **G. Zhao**[3], **J.-F. Deü**[2], **C. Collette**[3], **G. Kerschen**[1]
[1] Department of Aerospace and Mechanical Engineering, University of Liège,
Allée de la Découverte 9, 4000 Liege, Belgium
e-mail: **G.Raze@uliege.be**

[2] Laboratoire de Mécanique des Structures et des Systèmes Couplés, Conservatoire national des arts et métiers, 292 Rue Saint-Martin, 75003 Paris, France

[3] Department of Bio-, Electro- and Mechanical Systems, Precision Mechatronics Laboratory, Université Libre de Bruxelles, Av. F.D Roosevelt 50, 1050 Brussels, Belgium

Abstract
This paper presents a design methodology for a piezoelectric vibration absorber able to damp multiple nonlinear resonances. The design of multimodal linear piezoelectric absorbers is first reviewed. Next, based on the dynamics of the structure to which linear absorbers are attached, the design is extended to the nonlinear regime. The methodology is inspired from a principle of similarity: if a nonlinearity of one type is present in the host structure, the same type of nonlinearity is used in the absorbers. An explicit semi-analytical expression of the nonlinear coefficients in the absorber is obtained thanks to a first-order harmonic balance and a straightforward series expansion. Numerical examples are analysed to demonstrate the efficiency of the proposed approach.

1 Introduction

Owing to stringent requirements on performance, low-emission regulations and increasing price of energy, mechanical structures in the aerospace industry are becoming more lightweight, which makes them prone to experience high-amplitude vibrations. These structures can be subjected to broadband or multiharmonic forcing excitations. For sufficiently high forcing amplitudes, the induced motion can trigger nonlinearities such as geometric nonlinearities, contact or friction in bolted connections.

Among the existing possibilities for vibration mitigation, the piezoelectric vibration absorber appears as an attractive option: it does not include additional moving parts, the absorption system can be localised away from the points where the vibratory amplitude is critical and it eases the implementation of semi-active control. The first use of a piezoelectric vibration absorber is attributed to Forward [1]. Hagood and von Flotow [2] later provided design rules for piezoelectric shunts. Ever since that pioneering work, there has been a growing body of literature on the subject.

Real-life structures exhibit multiple resonances. If the excitation spectrum is not localised around a specific frequency, several modes can be excited simultaneously. Edberg et al [3] first proposed a two-mode shunt circuit connected to a single piezoelectric patch to damp simultaneously two structural modes. Hollkamp [4] later generalised it to any number of modes. The circuit of Hollkamp is unfortunately not easy to tune. Wu [5] proposed a multimodal current blocking shunt circuit with an associated design methodology. Despite its efficiency, the number of required electrical components grows quadratically with respect to the number of mode to be controlled. It makes the use of this circuit impractical for a large number of modes. Behrens et al [6] proposed a simplified multimodal current flowing shunt circuit, requiring one RLC branch per mode to be damped. Interestingly, another approach involving the connection of a mechanical structure to its

electrical analogue through multiple piezoelectric patches can serve the same purpose, as done by Lossouarn et al [7].

A linear absorber is detuned when nonlinearities arise due to high forcing amplitudes, and its performance might be substantially reduced. Through the intentional and adequate use of nonlinearities in the absorber, this detrimental effect can be significantly mitigated. Habib and Kerschen [8] showed that the design of a general nonlinear vibration absorber can be guided by a principle of similarity. This principle states that the mathematical form of the nonlinearity in the absorber should be identical to that of the primary structure. The range of forcing amplitudes in which the absorber is efficient can therefore be extended. Soltani and Kerschen [9] applied successfully this principle to a single-mode piezoelectric absorber, the nonlinear piezoelectric tuned vibration absorber (NPTVA), which was later experimentally realised by Lossouarn et al [10].

This paper brings together the multimodal and nonlinear aspects and proposes a multimodal nonlinear piezoelectric vibration absorber for the mitigation of multiple nonlinear resonances of mechanical systems using a single piezoelectric transducer. Nonlinearities are located in a shunt circuit with multiple branches, each tuned to a specific resonance frequency. The electrical nonlinearities are implemented using nonlinear capacitors. Their mathematical form is chosen thanks to a principle of similarity. An explicit expression of the nonlinear coefficients is obtained with a first-order harmonic balance method followed by a series expansion. The resulting absorber is able to effectively damp several nonlinear resonances.

2 Linear piezoelectric vibration absorber

This section briefly reviews the concepts of single-mode and multi-mode piezoelectric vibration absorbers. The linear absorbers are designed independently of the nonlinearities in the primary structure, and serve as a baseline for the design of nonlinear absorbers.

2.1 Single-mode piezoelectric vibration absorber

The purpose of a single-mode vibration absorber is to mitigate the vibration of its host structure. In Figure 1(a), the host structure is represented by a modal spring k and a modal mass m. The classical resonant shunt, as studied by Hagood and von Flotow [2], consists in connecting an series RL circuit to the electrodes of a piezoelectric material (in this case a piezoelectric stack) as shown in Figure 1(b). The piezoelectric material is a transducer, and is represented by both a mechanical and an electrical model. Mechanically, it behaves as a spring $k_{p,oc}$ (the stiffness of the piezoelectric element when its electrodes are open-circuited) in parallel with a force source f_p proportional to the charge in the piezoelectric element (Figure 1(a)). Electrically, it may be represented as a voltage source V_p proportional to the strain in the piezoelectric material in series with a capacitor C_p^ε (the capacitance of the piezoelectric material at constant strain). By connecting an inductor L and a resistor R to the electrodes of the piezoelectric material, a resonant RLC circuit is therefore created (Figure 1(b)). The tuning of the inductance and resistance is made according to the objectives at stake. The most common objectives include the minimisation of the H_∞ norm of the receptance [11] or the maximisation of modal damping [2].

2.2 Multimodal piezoelectric vibration absorber

One of the interesting features of the piezoelectric vibration absorber is that it can simultaneously mitigate the vibration of several modes of different frequencies if properly designed. Among the proposed approaches in the literature, one of the simplest is the current flowing shunt circuit proposed by Behrens et al [6]. This circuit is depicted in Figure 2. It consists in N resonant RLC branches, each tuned to a specific mode. It can resonate at N different frequencies, providing the possibility for multimodal shunt damping with a single piezoelectric transducer.

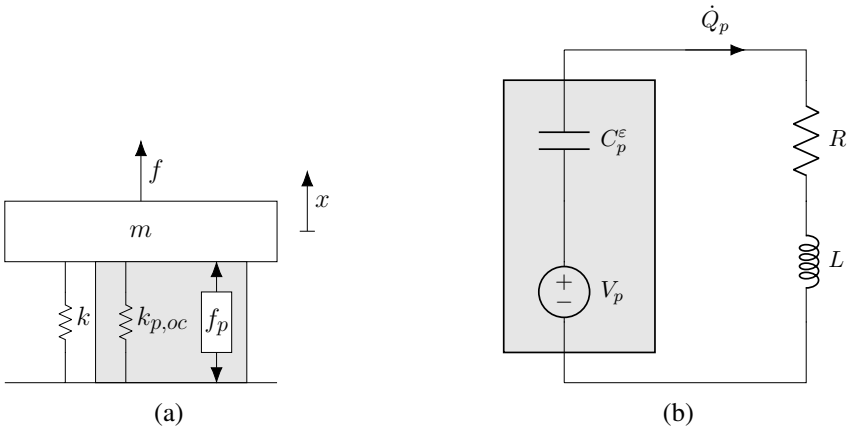

Figure 1: Single-mode resonant piezoelectric shunt: mechanical representation (a) and electrical representation (b).

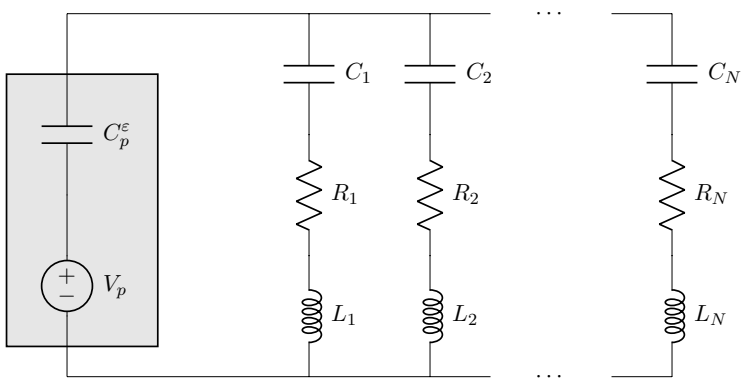

Figure 2: Current flowing shunt circuit.

The tuning methodology for this circuit relies on a model such as the one developed in the next subsection, and is therefore postponed to Subsection 2.4.

2.3 Model of a piezoelectric structure

A model of coupled second-order ordinary differential equations of the coupled electromechanical system is now derived. This model is necessary for the design of the absorbers, as discussed in the next subsection. The dynamics of the piezoelectric structure is governed by the following linear ordinary differential equations

$$\mathbf{M}_s\ddot{\mathbf{x}}_s + \mathbf{C}_s\dot{\mathbf{x}}_s + \mathbf{K}_s\mathbf{x}_s = \mathbf{f}_s + \mathbf{f}_p, \tag{1}$$

in which $\mathbf{M}_s$, $\mathbf{C}_s$ and $\mathbf{K}_s$ are the structural mass, damping and stiffness matrices (including the mechanical characteristics of the piezoelectric material), respectively, $\mathbf{x}_s$ is the vector of generalised degrees of freedom, $\mathbf{f}_s$ is the vector of generalised loading and $\mathbf{f}_p$ represents the generalised loading generated by the force source in the piezoelectric element. If Q_p is the charge in the piezoelectric material, this loading is given by

$$\mathbf{f}_p = \theta_p\mathbf{B}_pQ_p, \tag{2}$$

where $\mathbf{B}_p$ is an influence vector [12] and θ_p is a piezoelectric coupling coefficient. Since all the branches of the current flowing circuit are in parallel, they are subjected to the same voltage difference V. Then, if q_i is

the electrical charge in the i^{th} branch,

$$L_i\ddot{q}_i + R_i\dot{q}_i + \frac{1}{C_i}q_i = V_i = V, \qquad \forall i \in [1, ..., N], \tag{3}$$

where L_i, R_i and C_i respectively are the inductance, resistance and capacitance of the i^{th} branch of the current flowing circuit represented in Figure 2. The voltage difference V is also the voltage across the electrodes of the piezoelectric material. It is given by the strain-driven voltage source of the piezoelectric material V_p, minus the voltage drop across the piezoelectric capacitance $V_{C_p^\varepsilon}$.

$$V = V_p - V_{C_p^\varepsilon} = \theta_p \mathbf{B}_p^T \mathbf{x}_s - \frac{1}{C_p^\varepsilon} Q_p \tag{4}$$

The superscript T denotes a transposition. Charge conservation imposes the following equality

$$Q_p = \sum_{i=1}^{N} q_i. \tag{5}$$

Combining Equations (3), (4) and (5) and introducing the vector of electric charges $\mathbf{x}_e = [q_1, ..., q_N]^T$ yields

$$\mathbf{M}_e\ddot{\mathbf{x}}_e + \mathbf{C}_e\dot{\mathbf{x}}_e + \mathbf{K}_e\mathbf{x}_e = \theta_p \mathbf{1}_{N\times 1}\mathbf{B}_p^T\mathbf{x}_s = \mathbf{\Theta}\mathbf{x}_s, \tag{6}$$

in which $\mathbf{M}_e$, $\mathbf{C}_e$ and $\mathbf{K}_e$ are the electrical mass, damping and stiffness matrices, respectively, given by

$$\mathbf{M}_e = \mathbf{diag}([L_1, ..., L_N]), \tag{7}$$

$$\mathbf{C}_e = \mathbf{diag}([R_1, ..., R_N]), \tag{8}$$

$$\mathbf{K}_e = \mathbf{diag}\left(\left[\frac{1}{C_1}, ..., \frac{1}{C_N}\right]\right) + \frac{1}{C_p^\varepsilon}\mathbf{1}_{N\times N}, \tag{9}$$

$\mathbf{1}_{m\times n}$ is a matrix of size $m \times n$ filled with ones and $\mathbf{\Theta}$ is an electromechanical coupling matrix. Eventually, a system of coupled electromechanical equations is obtained by combining Equations (1), (2) and (6).

$$\begin{bmatrix} \mathbf{M}_s & \mathbf{0} \\ \mathbf{0} & \mathbf{M}_e \end{bmatrix} \begin{bmatrix} \ddot{\mathbf{x}}_s \\ \ddot{\mathbf{x}}_e \end{bmatrix} + \begin{bmatrix} \mathbf{C}_s & \mathbf{0} \\ \mathbf{0} & \mathbf{C}_e \end{bmatrix} \begin{bmatrix} \dot{\mathbf{x}}_s \\ \dot{\mathbf{x}}_e \end{bmatrix} + \begin{bmatrix} \mathbf{K}_s & -\mathbf{\Theta}^T \\ -\mathbf{\Theta} & \mathbf{K}_e \end{bmatrix} \begin{bmatrix} \mathbf{x}_s \\ \mathbf{x}_e \end{bmatrix} = \begin{bmatrix} \mathbf{f}_s \\ \mathbf{0} \end{bmatrix}. \tag{10}$$

Equation (10) may be written in a more compact form

$$\mathbf{M}\ddot{\mathbf{x}} + \mathbf{C}\dot{\mathbf{x}} + \mathbf{K}\mathbf{x} = \mathbf{f}, \tag{11}$$

with $\mathbf{x}^T = [\mathbf{x}_s^T \ , \ \mathbf{x}_e^T]$.

2.4 Design of the electrical circuit

In the current flowing circuit proposed by Behrens et al [6], one of the electrical elements of each branch can be chosen arbitrarily. In that paper, the choice of the filter capacitances is arbitrary, the tuning of the inductances of the current flowing circuit is straightforward, and the tuning of the resistances requires an optimisation algorithm as the one proposed by Fleming et al [13]. However, no explanation was given on the impact of the choice of the filter capacitances. The effect of placing a parallel capacitance across the terminals of the piezoelectric material was shown to influence the damping performance of a single-mode shunt circuit by Fleming et al [14]. The subsequent work of Cigada et al [15] highlighted the influence of the filter capacitances in the case of the current flowing circuit. They showed that a higher filter capacitance enables a better control capability on the mode it is associated to. Unfortunately, increasing the filter capacitance also increases the coupling between the different branches of the circuit. It was shown that the tuning rule of [6] started to fail as the filter capacitances were increased because of this increased coupling. An optimisation algorithm was also proposed in that paper to tune the inductances so as to set the resonance frequencies of the circuit properly.

In this paper, the choice of the filter capacitance is made beforehand, and a two-step optimisation algorithm is used to tune the remaining electrical parameters. First, following the proposition of Cigada et al [15], the inductances are tuned so that the undamped electrical circuit (the circuit without resistors) has the desired resonance frequencies. In the case of multimodal shunt damping, these resonance frequencies should match these of the structural modes that have to be damped. Then, the resistances are computed using the optimisation algorithm proposed in [13].

For the first step of the algorithm, the cost function is defined as

$$f(L_1, ..., L_N) = \sum_{i=1}^{N} (\omega_{e,i}^2 - \omega_{s,i}^2)^2, \tag{12}$$

where $\omega_{e,i}$ is the i^{th} resonance frequency of the electrical circuit and $\omega_{s,i}$ is its targeted value. Since the square of $\omega_{e,i}$ are the eigenvalues of the matrix $\mathbf{M}_e^{-1}\mathbf{K}_e$, their sensitivity to the inductance L_j can be computed analytically (Van der Aa et al [16]) as

$$\frac{\partial \omega_{e,i}^2}{\partial L_j} = -\mathbf{\Phi}_e^{-1}\mathbf{M}_e^{-1}\frac{\partial \mathbf{M}_e}{\partial L_j}\mathbf{M}_e^{-1}\mathbf{K}_e\mathbf{\Phi}_e, \tag{13}$$

where $\mathbf{\Phi}_e$ is the matrix of right eigenvectors of $\mathbf{M}_e^{-1}\mathbf{K}_e$. The sensitivity of the cost function is then

$$\frac{\partial f}{\partial L_j} = 2\sum_{i=1}^{N}(\omega_{e,i}^2 - \omega_{s,i}^2)\frac{\partial \omega_{e,i}^2}{\partial L_j}. \tag{14}$$

With this formulation, an unconstrained optimisation algorithm can readily be used. Once the resonance frequencies of the undamped electrical circuit are tuned, the second step of the algorithm consists in tuning the resistances values with the algorithm proposed in [13]. This algorithm is based on a state-space model of the whole structure and aims at minimising the H_2 norm of the receptance. With the model proposed in Subsection 2.3, the state-space matrices $\tilde{\mathbf{A}}$ and $\tilde{\mathbf{B}}$ can be readily built:

$$\tilde{\mathbf{A}} = \begin{bmatrix} \mathbf{0} & \mathbf{I} \\ -\mathbf{M}^{-1}\mathbf{K} & -\mathbf{M}^{-1}\mathbf{C} \end{bmatrix}, \qquad \tilde{\mathbf{B}} = \begin{bmatrix} \mathbf{0} \\ \mathbf{M}^{-1}\mathbf{f} \end{bmatrix}. \tag{15}$$

The state-space matrix $\tilde{\mathbf{C}}$ is chosen according to the choice of the degree of freedom at which the H_2 norm of the transfer function has to be minimised. The three state-space matrices can then be used in the algorithm of [13].

Another objective for the choice of the resistances could have been the optimisation of the H_∞ norm of the receptance, yielding the so-called equal-peak design. This kind of optimisation is often harder to accomplish than the H_2 optimisation and is beyond the scope of this paper. Nevertheless, the H_2 optimisation algorithm can provide nearly-equal peaks and is not that far from the H_∞ optimum.

3 Nonlinear piezoelectric vibration absorber

Real-life structures often depart from their ideal linear behaviour as the forcing amplitude increases. The inherent nonlinearities in the primary structure might have undesirable effects on the performance of the absorbers. Using nonlinearities in the absorbers as well can benefit their performance. This section proposes a design methodology for these nonlinear absorbers. It is assumed that the linear absorbers have already been tuned.

3.1 A principle of similarity

In [8], the authors showed that an intentional and adequate use of nonlinearities in a vibration absorber coupled to a nonlinear structure could substantially improve its performance. The nonlinearities have to be chosen according to a principle of similarity: they should have the same mathematical form as those of the primary structure.

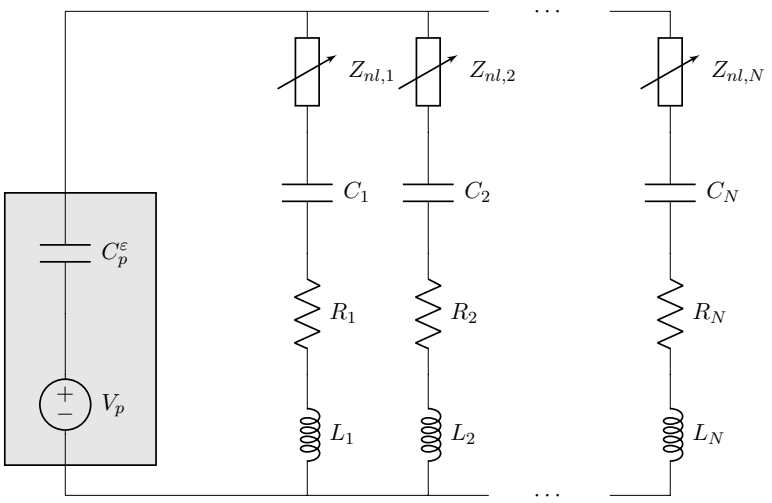

Figure 3: Nonlinear current flowing shunt circuit.

Figure 3 depicts the general arrangement of a nonlinear current flowing circuit. Essentially nonlinear impedances are considered to reflect the effect of the nonlinearities in the primary structure. Their arbitrary placement is guided by the behaviour of the linear current flowing circuit. It is expected that each nonlinear impedance will have a pronounced effect on the mode to which its branch is tuned. The physical type of the nonlinear impedance is made depending on practical considerations such as availability of the components. For instance, a nonlinear stiffness may be controlled with a nonlinear capacitor [9]. Another possibility is to use saturable inductors as in [10]. Once the type of nonlinear components has been chosen, it is necessary to determine their coefficients. In the following sections, a design methodology is proposed.

3.2 Nonlinear frequency response

Using the same formalism as Habib and Kerschen [17], the coupled nonlinear electromechanical equations are

$$\mathbf{M}\ddot{\mathbf{x}} + \mathbf{C}\dot{\mathbf{x}} + \mathbf{K}\mathbf{x} + k_{nl}\left(\mathbf{b}_{nl}(\mathbf{x}) + \sum_{i=1}^{N} b_{nl,i}\mathbf{b}_{nl,i}(\mathbf{x})\right) = \mathbf{f}(t), \tag{16}$$

where $\mathbf{b}_{nl}$ represents the nonlinearities in the primary structure, and $\mathbf{b}_{nl,i}$ are the nonlinearities in the absorbers. According to the principle of similarity, the latter are chosen to have the same mathematical form as the former. In the following, it is assumed that the nonlinearities are cubic. The remaining unknowns are the nonlinear coefficients of the absorbers, $b_{nl,i}$.

The coupled electromechanical equations are normalised considering $\mathbf{y} = \mathbf{x}/f_0$

$$\mathbf{M}\ddot{\mathbf{y}} + \mathbf{C}\dot{\mathbf{y}} + \mathbf{K}\mathbf{y} + \alpha_3\left(\mathbf{b}_{nl}(\mathbf{y}) + \sum_{i=1}^{N} b_{nl,i}\mathbf{b}_{nl,i}(\mathbf{y})\right) = \frac{\mathbf{f}(t)}{f_0}, \tag{17}$$

in which $\alpha_3 = k_{nl}f_0^2$ for cubic nonlinearities. The nonlinearity parameter α_3 quantifies the effects of both the nonlinearity and the forcing. The solution of Equation (17) under a harmonic forcing can be approximated with a first-order harmonic balance (HB) method. Using

$$\mathbf{y} = \mathbf{q}_c\cos(\omega t) + \mathbf{q}_s\sin(\omega t), \tag{18}$$

and introducing $\mathbf{q}^T = [\mathbf{q}_c^T, \mathbf{q}_s^T]$, Equation (17) becomes

$$\mathbf{W}\mathbf{q} + \alpha_3\left(\mathbf{d}_{1,nl}(\mathbf{q}) + \sum_{i=1}^{N} b_{nl,i}\mathbf{d}_{1,nl,i}(\mathbf{q})\right) = \mathbf{c}. \tag{19}$$

In Equation (19), the matrix $\mathbf{W}$ represents the linear dynamics, $\mathbf{c}$ is the forcing term, and the terms $\mathbf{d}_{1,nl}$ and $\mathbf{d}_{1,nl,i}$ represent the nonlinearities in the primary structure and in the i^{th} absorber, respectively. Thanks to the HB method, Equation (17), representing a set of nonlinear ordinary differential equations, has been transformed into a set of nonlinear algebraic equations. To find an approximate solution, it is further assumed that the nonlinearity parameter α_3 is small. Hence, the nonlinear response of the system may be expressed as a series expansion in terms of α_3 as

$$\mathbf{q} = \mathbf{q}^{(0)} + \alpha_3\mathbf{q}^{(1)} + \alpha_3^2\mathbf{q}^{(2)} + O(\alpha_3^3). \tag{20}$$

Inserting Equation (20) into (19) and equating coefficients of like powers of α_3 up to first order leads to the following explicit relations :

$$\mathbf{q}^{(0)} = \mathbf{W}^{-1}\mathbf{c}, \tag{21}$$

$$\mathbf{q}^{(1)} = -\mathbf{W}^{-1}\left(\mathbf{d}_{1,nl}(\mathbf{q}^{(0)}) + \sum_{i=1}^{N} b_{nl,i}\mathbf{d}_{1,nl,i}(\mathbf{q}^{(0)})\right) = \mathbf{q}_{nl}^{(1)} + \sum_{i=1}^{N} b_{nl,i}\mathbf{q}_{nl,i}^{(1)}. \tag{22}$$

Equation (21) indicates that $\mathbf{q}^{(0)}$ represents the response of the system when no nonlinearity is present. Equation (22) shows that first-order terms $\mathbf{q}^{(1)}$ are generated by the nonlinear forces triggered by the zeroth-order motion. These terms can be separated into terms due to the nonlinearities inside the primary structure

$\mathbf{q}_{nl}^{(1)}$ and terms due to the nonlinearities inside the i^{th} absorber $\mathbf{q}_{nl,i}^{(1)}$. The square of the frequency response function at a given degree of freedom is given by

$$H = \left(\mathbf{q}_c\right)_j^2 + \left(\mathbf{q}_s\right)_j^2 . \tag{23}$$

Inserting the solution of (21) and (22) into (23) and keeping only the first-order terms leads to

$$\begin{aligned} H &= \left(\mathbf{q}_c^{(0)}\right)_j^2 + \left(\mathbf{q}_s^{(0)}\right)_j^2 + \alpha_3 \left[2\left(\mathbf{q}_c^{(0)}\right)_j \left(\mathbf{q}_{c,nl}^{(1)}\right)_j + 2\left(\mathbf{q}_s^{(0)}\right)_j \left(\mathbf{q}_{s,nl}^{(1)}\right)_j\right] \\ &\quad + \alpha_3 \left[\sum_{i=1}^{N} b_{nl,i} \left[2\left(\mathbf{q}_c^{(0)}\right)_j \left(\mathbf{q}_{c,nl,i}^{(1)}\right)_j + 2\left(\mathbf{q}_s^{(0)}\right)_j \left(\mathbf{q}_{s,nl,i}^{(1)}\right)_j\right]\right] \\ &= H^{(0)} + \alpha_3 H_{nl}^{(1)} + \alpha_3 \sum_{i=1}^{N} b_{nl,i} H_{nl,i}^{(1)} \end{aligned} . \tag{24}$$

In Equation (24), three terms can be identified. The term $H^{(0)}$ stands for the frequency response function of the underlying linear structure. The term $\alpha_3 H_{nl}^{(1)}$ is the modification brought by the (supposedly small) nonlinear forces generated by the linear motion in the nonlinearities of the primary structure. The term $\alpha_3 b_{nl,i} H_{nl,i}^{(1)}$ is the modification brought by the (supposedly small) nonlinear forces generated by the linear motion in the nonlinearitiy i of the absorbers. Thanks to the straightforward expansion, all these effects can be separated to first order in α_3.

With Equation (24), it is now possible to impose N conditions on the first-order nonlinear FRF. This yields a linear system of size $N \times N$, where the nonlinear coefficients $b_{nl,i}$ are the unknowns. Depending on the imposed conditions, the nonlinear coefficients may or may not depend on the parameter α_3.

3.3 Imposing equal peaks in the nonlinear regime

A condition enforcing equal peaks in the nonlinear regime will now be derived. It is first assumed that in the linear regime, the linear absorbers yield the so-called equal-peak design, i. e. the peaks are equal in magnitude and located at frequencies $\omega_{j,p1}$ and $\omega_{j,p2}$. Equation (24) can be used to enforce the equality of the first-order nonlinear FRFs.

$$\begin{aligned} &H^{(0)}(\omega_{j,p1}) + \alpha_3 \left(H_{nl}^{(1)}(\omega_{j,p1}) + \sum_{i=1}^{N} b_{nl,i} H_{nl,i}^{(1)}(\omega_{j,p1})\right) \\ &= H^{(0)}(\omega_{j,p2}) + \alpha_3 \left(H_{nl}^{(1)}(\omega_{j,p2}) + \sum_{i=1}^{N} b_{nl,i} H_{nl,i}^{(1)}(\omega_{j,p2})\right) \end{aligned} \tag{25}$$

Since equal peaks were assumed in the linear regime, $H^{(0)}(\omega_{j,p1}) = H^{(0)}(\omega_{j,p2})$. Then, Equation (25) becomes independent of α_3 and can be written as

$$\sum_{i=1}^{N} b_{nl,i} \left(H_{nl,i}^{(1)}(\omega_{j,p1}) - H_{nl,i}^{(1)}(\omega_{j,p2})\right) = H_{nl}^{(1)}(\omega_{j,p2}) - H_{nl}^{(1)}(\omega_{j,p1}). \tag{26}$$

Enforcing Equation (26) for $j = 1, \cdots, N$ yields the following linear system of size $N \times N$:

$$\begin{bmatrix} \Delta_{\omega_1} H^{(1)}_{nl,1} & \Delta_{\omega_1} H^{(1)}_{nl,2} & \dots & \Delta_{\omega_1} H^{(1)}_{nl,N} \\ \Delta_{\omega_2} H^{(1)}_{nl,1} & \Delta_{\omega_2} H^{(1)}_{nl,2} & \dots & \vdots \\ \vdots & \vdots & \ddots & \vdots \\ \Delta_{\omega_N} H^{(1)}_{nl,1} & \dots & \dots & \Delta_{\omega_N} H^{(1)}_{nl,N} \end{bmatrix} \begin{bmatrix} b_{nl,1} \\ b_{nl,2} \\ \vdots \\ b_{nl,N} \end{bmatrix} = - \begin{bmatrix} \Delta_{\omega_1} H^{(1)}_{nl} \\ \Delta_{\omega_2} H^{(1)}_{nl} \\ \vdots \\ \Delta_{\omega_N} H^{(1)}_{nl} \end{bmatrix}, \tag{27}$$

in which

$$\Delta_{\omega_j} H = H(\omega_{j,p1}) - H(\omega_{j,p2}). \tag{28}$$

Note that the equality of the peaks in the linear regime is not strictly necessary for the absorbers to work efficiently. Indeed, Equation (26) expresses that the (first-order) effects of all the nonlinearities is the same at $\omega_{j,p1}$ and $\omega_{j,p2}$. Therefore, if the peaks are only approximately equal in the linear regime (which is the case with the H_2 optimisation), they will remain approximately equal in the nonlinear regime.

Because the frequency response (24) is only accurate to the first order, this approach is a local approach, in the sense that the obtained results will gradually lose their validity with increasing α_3. That is, if either the forcing amplitude or the nonlinear coefficients become large, the proposed method is likely to fail. For small α_3 however, it is expected that the nonlinear absorbers yield better result than their linear counterparts.

4 Numerical examples

The proposed approach is illustrated with two numerical examples. The frequency response functions were computed using a continuation procedure coupled with a harmonic balance formalism [18] with five harmonics.

4.1 Comparison with the Nonlinear Piezoelectric Tuned Vibration Absorber

As a verification of the proposed method, it is compared to the NPTVA proposed by Soltani and Kerschen [9]. In that paper, the nonlinearities in the absorber are chosen according to a principle of similarity as well. Their coefficients are determined thanks to a first-order HB and a homotopy perturbation method.

A single-degree-of-freedom structure to which a piezoelectric stack is attached (Figure 1) is considered as an example. A nonlinear cubic spring is attached to the mass as well. The piezoelectric stack is connected to a shunt circuit in an attempt to mitigate the vibrations. The coupling between the structure and the piezoelectric material can be characterised by the effective electromechanical coupling factor (EEMCF) defined as [19]

$$K_c^2 = \frac{\omega_{oc}^2 - \omega_{sc}^2}{\omega_{sc}^2}, \tag{29}$$

where ω_{oc} is the resonance frequency of the structure when the electrodes of the piezoelectric material are open-circuited and ω_{sc} is the resonance frequency of the structure when these electrodes are short-circuited. In this example, the numerical parameters are given in Table 1. The EEMCF is varied between 0.05 and 0.6. The optimal inductance and resistance of the linear piezoelectric shunt are computed following [11]. The nonlinear impedances are implemented with cubic capacitances. The electromechanical equations are given by

m	k	$k_{p,oc}$	k_{nl}	C_p^ε
1 kg	0.5 N/m	0.5 N/m	1 N/m^3	1 F

Table 1: Numerical parameters of the single-degree-of-freedom structure.

$$\begin{cases} m\ddot{x} + (k + k_{p,oc})x + k_{nl}x^3 - \theta_p q = f \\ L\ddot{q} + R\dot{q} + \dfrac{1}{C_p^\varepsilon} q + C_{nl}q^3 - \theta_p x = 0 \end{cases} . \tag{30}$$

The nonlinear coefficients computed using the method in [9] and the method proposed in Subsection 3 are compared.

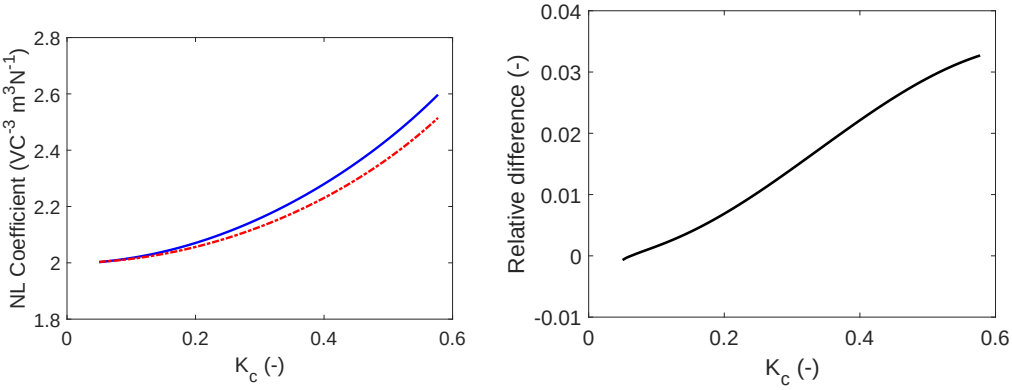

(a) (b)

Figure 4: Comparison of the NPTVA (—) and the proposed method (– · –): nonlinear coefficients (a) and relative difference between the coefficients (b).

Figure 4 shows a comparison between the results of the proposed method and the NPTVA (a forcing amplitude of 10^{-3} N was chosen to account for the local nature of the proposed approach, and a modal damping of 1% in the host structure was assumed). A good agreement between the computed nonlinear coefficients is observed, with up to 3% relative difference for the highest coupling factor (the coefficient m_3 of the NPTVA as given in [9] has to be multiplied by $(L/m)^2$ to have consistent units). For realistic EEMCFs, that is $K_c \leq 0.2$, the relative difference is less than 1%.

Next, the EEMCF is fixed to $K_c = 0.2$ and the forcing amplitude is varied. Figure 5 shows the nonlinear frequency responses functions (NFRF) of the system with only a linear absorber, with the NPTVA and with the absorber tuned according to Subsection 3. As the hardening effects of the nonlinearity inside the structure become more prominent, the linear absorber is progressively detuned and loses its efficiency. Around $f = 0.0416$, a detached resonance curve (DRC) merges with the rightmost peak of the NFRF, leading to the possibility of high-amplitude vibrations over a broad frequency range. On the other hand, the nonlinear absorbers are able to mitigate the vibrations over a larger range of forcing amplitudes. Indeed, the difference between the maximum of the receptance with and without nonlinear absorbers is 15.73 dB at $f = 0.05$.

4.2 Two-degree-of-freedom structure

To demonstrate the ability of the method to damp multiple modes, a two-degree-of-freedom structure shown in Figure 6 is studied. A cubic spring k_{nl} attached to mass 1 is considered to introduce nonlinear effects. The characteristics of the structure as well as those of the piezoelectric stack are given in Table 2 (where $K_{c,1}$

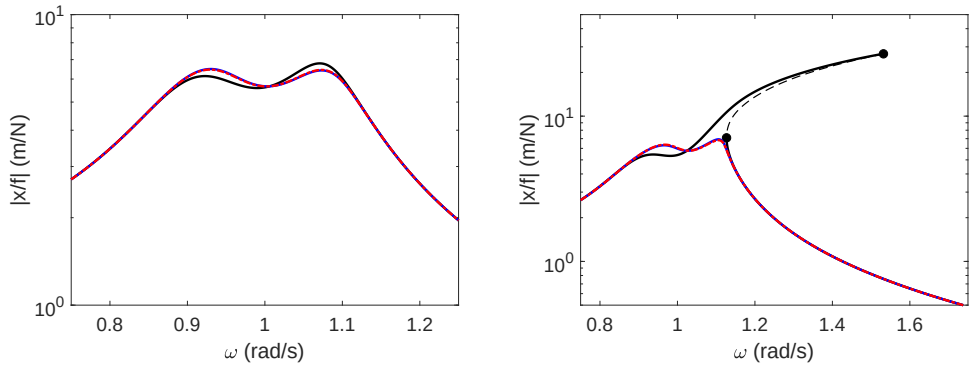

Figure 5: Comparison of the NPTVA and the proposed method: nonlinear frequency response function at $f = 0.025$ N (a) and $f = 0.05$ N (b): linear absorbers (—: stable solution, - - : unstable solution, •: fold bifurcation), NPTVA (—) and the proposed approach (– · –).

and $K_{c,2}$ are the EEMCFs of modes 1 and 2, respectively). Damping is also introduced to have 1% modal damping on both modes in the primary structure. The structure is subjected to a harmonic forcing located on the first mass and the displacement is measured as this same mass.

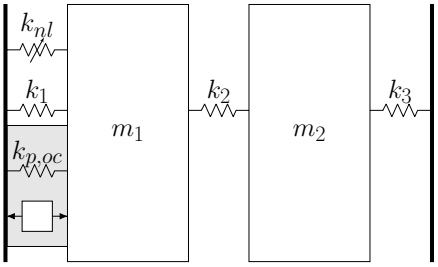

Figure 6: Two-degree-of-freedom structure.

m_1	m_2	k_1	k_2	k_3	k_{nl}	$k_{p,oc}$	C_p^ε	$K_{c,1}$	$K_{c,2}$
1 kg	1 kg	5 N/m	5 N/m	1 N/m	1 N/m^3	1 N/m	1 F	0.0774	0.0567

Table 2: Numerical parameters of the two-degree-of-freedom structure.

A two-mode current flowing shunt circuit is connected to the electrodes of the piezoelectric stack. The choice of the filter capacitances was made empirically so as to obtain approximately the same amplitude on both modes. The inductances values are initialised using the simple rule in [6]. The inductances and resistances are then tuned using the two-step algorithm described in Subsection 2.4. The obtained parameters are gathered in Table 3. The amplitude reductions of modes 1 and 2 are 16.9 dB and 18.6 dB respectively.

Figure 7 illustrates the different steps of the design algorithm with the receptance of the structure in the linear regime. It can be seen that the initialisation of the inductances provides a circuit whose resonance frequencies are not correctly tuned to those of the structure. After a correction of the inductances, the resistances are optimised to minimise the H_2 norm of the receptance.

Nonlinear cubic capacitances are then added in each branch of the current flowing shunt circuit. Their coefficient is determined using Equation (27) and is given in Table 3. The NFRFs of the structure with and without nonlinearities in the absorber are compared in Figure 8 (mode 1) and Figure 9 (mode 2) for various forcing amplitudes.

Once again, the nonlinear absorbers are able to mitigate the vibration amplitude over a broader range of

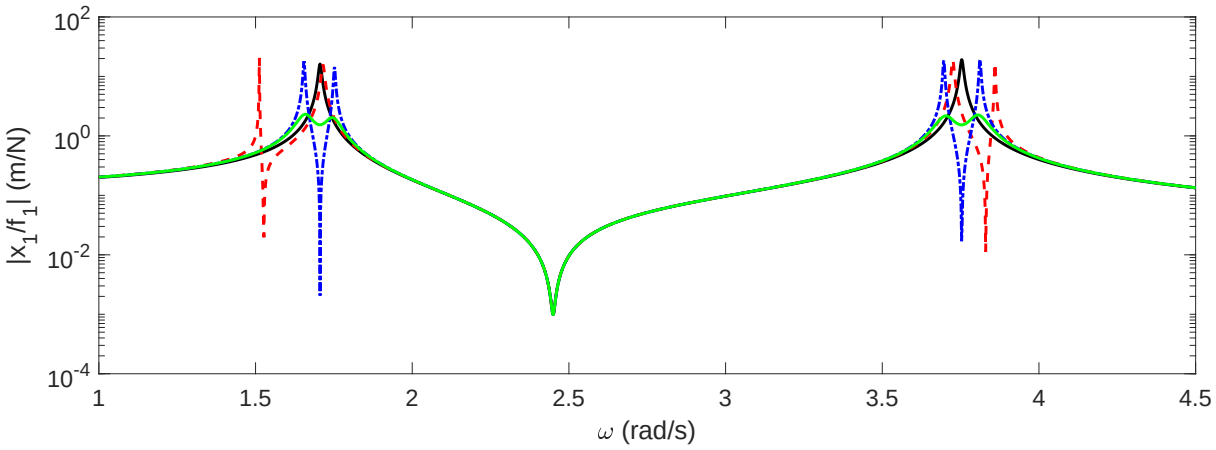

Figure 7: Steps of the design algorithm for the linear absorbers: open-circuit piezoelectric stack (—), initial guess for the inductances of the undamped circuit (- -), optimised inductances of the undamped circuit (– · –) and final design (—).

C_1	C_2	R_1	R_2	L_1	L_2	$C_{nl,1}$	$C_{nl,2}$
5 F	0.25 F	0.0316 Ω	0.0438 Ω	0.3244 H	0.3759 H	0.0169 V/C^3	0.1524 V/C^3

Table 3: Parameters of the current flowing shunt circuit.

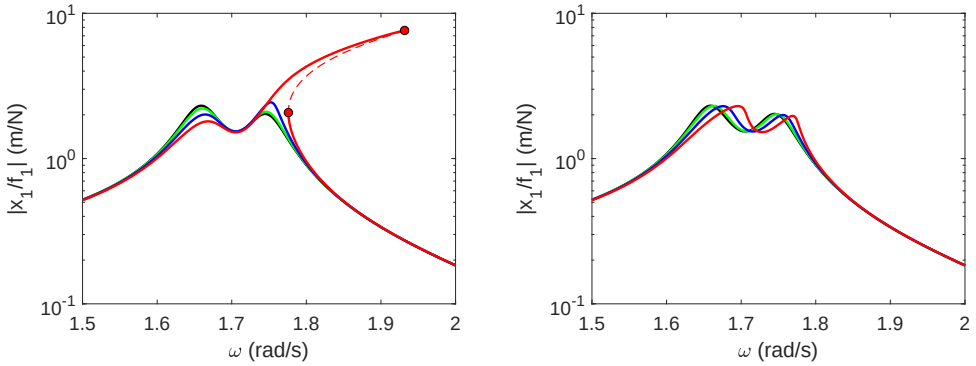

Figure 8: NFRFs of the structure with linear absorbers (a) and with nonlinear absorbers (b), close-up on mode 1: linear FRF (—), $f_1 = 0.1$ N (—), $f_1 = 0.2$ N (—), $f_1 = 0.3$ N (—: stable solution, - - : unstable solution, ●: fold bifurcation).

forcing amplitudes. Figure 8 shows that the proposed method yields nonlinear absorbers with fair efficiency even though the peaks resulting from the linear design are not perfectly equal in amplitude. In Figure 9(a), a DRC coalesced with the rightmost peak of mode 2 can be observed. The use of nonlinear absorbers delays this undesirable phenomenon to higher forcing amplitudes. A global view of the NFRF is given in Figure 10. This shows that both nonlinear resonances are damped simultaneously by the nonlinear absorbers.

The nonlinear absorbers are not fail-proof, though. At $f_1 = 0.3265$ N, a DRC merges with the rightmost peak of mode 2 with the nonlinear absorbers. At this point, the receptance amplitude around the frequency of mode 2 becomes comparable whether or not nonlinearities are used in the absorbers, as can be seen in Figure 11. This phenomenon bears a strong resemblance with that of the nonlinear tuned vibration absorber [20]. Nevertheless, mode 1 is still correctly damped with nonlinear absorbers.

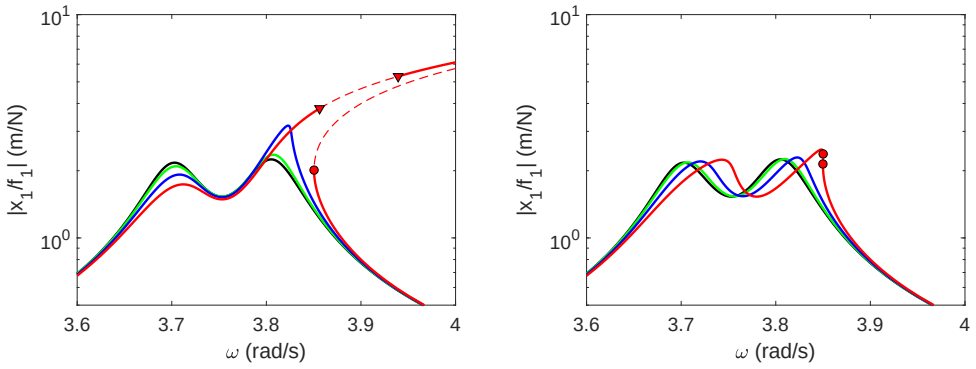

Figure 9: NFRFs of the structure with linear absorbers (a) and with nonlinear absorbers (b), close-up on mode 2: linear FRF (—), $f_1 = 0.1$ N (—), $f_1 = 0.2$ N (—), $f_1 = 0.3$ N (—: stable solution, - - : unstable solution, •: fold bifurcation, ▼: Neimark-Sacker bifurcation).

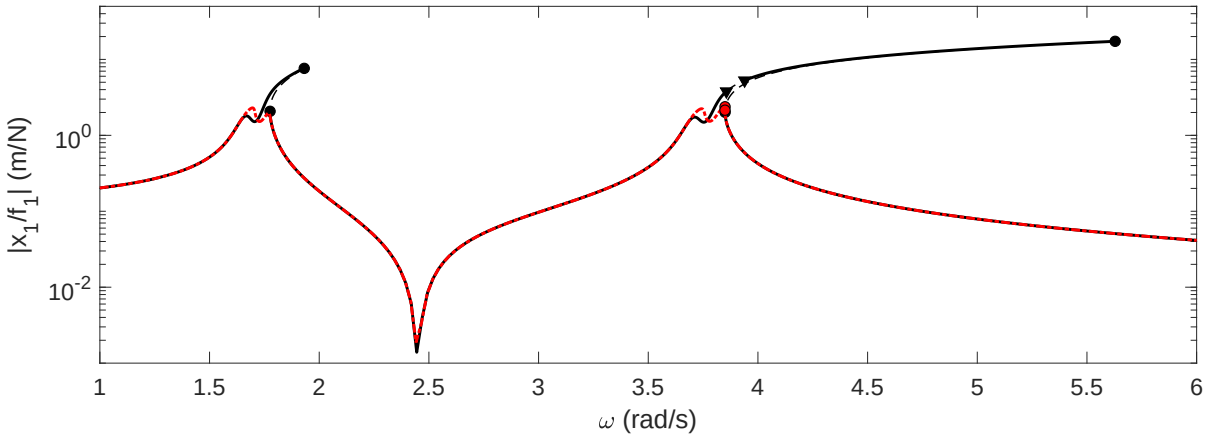

Figure 10: NFRF of the structure at $f_1 = 0.3$ N with linear absorbers (—: stable solution, - -: unstable solution, •: fold bifurcation, ▼: Neimark-Sacker bifurcation) and with nonlinear absorbers (— · — : stable solution, - -: unstable solution,•: fold bifurcation).

5 Conclusion

In this paper, a new methodology for tuning multimodal nonlinear piezoelectric vibration absorbers was proposed. A current flowing shunt circuit proposed in the literature was chosen to implement a multimodal absorber. A model of the piezoelectric structure connected to a current flowing shunt circuit was proposed, and this allowed us to revisit the tuning methodology of the shunt circuit. This methodology consists in a two-step optimisation algorithm. The inductances are first optimised to yield the correct resonance frequencies, and then the resistances are optimized to minimise the H_2 norm of the receptance.

The design of nonlinear multimodal vibration absorbers is inspired from a principle of similarity. Nonlinearities are introduced in the branches of the shunt circuit to mimic the behaviour of the structure in the nonlinear regime. Their mathematical form is chosen to be identical as these in the primary structure. Their coefficients are then found by imposing equal peaks in the nonlinear frequency response function.

The proposed design methodology was shown to be efficient both when a single mode and when two modes are to be damped. Namely, the range of forcing amplitudes in which the absorbers are efficient is substantially increased when properly tuned nonlinearities are used in the absorbers. Eventually, for very high forcing amplitudes, the nonlinear absorbers also fail and at that point the advantage of using nonlinearities becomes

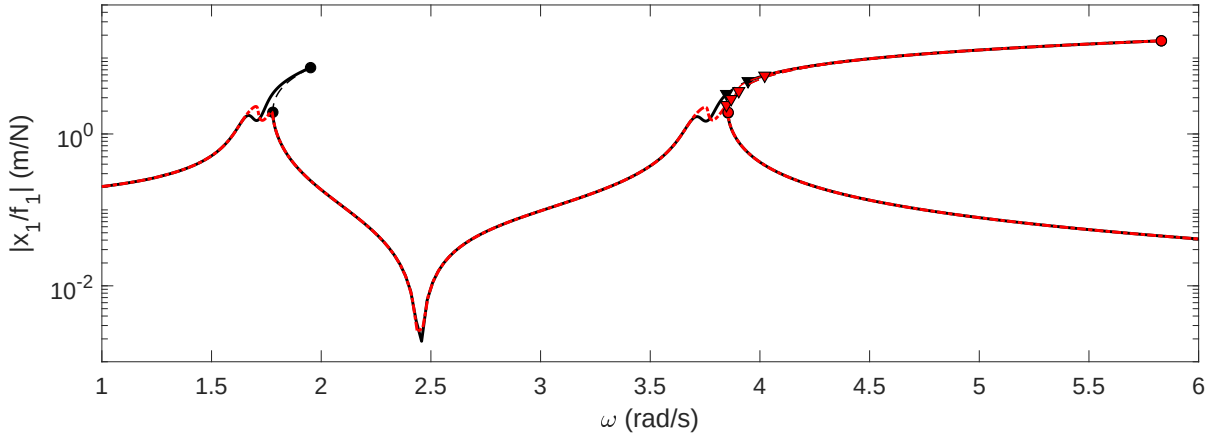

Figure 11: NFRFs of the structure at $f_1 = 0.3265$ N with linear absorbers (—: stable solution, - -: unstable solution, •: fold bifurcation, ▼: Neimark-Sacker bifurcation) and with nonlinear absorbers (– · – : stable solution, - -: unstable solution,•: fold bifurcation, ▼: Neimark-Sacker bifurcation).

less obvious.

The design of the nonlinearities relies on the presence of equal (or nearly equal) peaks in the linear receptance of the structure. Therefore, the design of linear absorbers has a strong impact on that of the nonlinearities. Future work for improving the proposed design methodology may involve choosing the inductances and the resistances in the objective of minimising the H_∞ norm of the receptance (and no longer its H_2 norm).

Acknowledgements

The authors G. Raze, A. Paknejad, G. Zhao, C. Collette and G. Kerschen would like to acknowledge the financial support of the SPW (WALInnov grant 1610122).

References

[1] R. L. Forward, *Electronic damping of vibrations in optical structures*, Applied optics, Vol. 18, No. 5, (1979), pp. 690–697.

[2] N. W. Hagood, A. von Flotow, *Damping of structural vibrations with piezoelectric materials and passive electrical networks*, Journal of Sound and Vibration, Vol. 146, No. 2, (1991), pp. 243–268.

[3] D. Edberg, A. Bicos, J. Fechter, *On piezoelectric energy conversion for electronic passive damping enhancement*, *Proceedings of Damping* (1991), pp. 717–724.

[4] J. J. Hollkamp, *Multimodal passive vibration suppression with piezoelectric materials and resonant shunts*, Journal of intelligent material systems and structures, Vol. 5, No. 1, (1994), pp. 49–57.

[5] S.-Y. Wu, *Method for multiple-mode shunt damping of structural vibration using a single PZT transducer*, *Smart structures and materials 1998: passive damping and isolation*, International Society for Optics and Photonics (1998), pp. 159–169.

[6] S. Behrens, S. R. Moheimani, A. Fleming, *Multiple mode current flowing passive piezoelectric shunt controller*, Journal of Sound and Vibration, Vol. 266, No. 5, (2003), pp. 929–942.

[7] B. Lossouarn, M. Aucejo, J.-F. Deü, *Multimodal coupling of periodic lattices and application to rod vibration damping with a piezoelectric network*, Smart Materials and Structures, Vol. 24, No. 4, (2015), p. 045018.

[8] G. Habib, G. Kerschen, *A principle of similarity for nonlinear vibration absorbers*, Physica D: Nonlinear Phenomena, Vol. 332, (2016), pp. 1–8.

[9] P. Soltani, G. Kerschen, *The nonlinear piezoelectric tuned vibration absorber*, Smart Materials and Structures, Vol. 24, No. 7, (2015), p. 075015.

[10] B. Lossouarn, J.-F. Deü, G. Kerschen, *A fully passive nonlinear piezoelectric vibration absorber*, Philosophical Transactions of the Royal Society of London A: Mathematical, Physical and Engineering Sciences (In Press).

[11] P. Soltani, G. Kerschen, G. Tondreau, A. Deraemaeker, *Piezoelectric vibration damping using resonant shunt circuits: an exact solution*, Smart materials and structures, Vol. 23, No. 12, (2014), p. 125014.

[12] A. Preumont, *Vibration control of active structures*, Springer (2011).

[13] A. J. Fleming, S. Behrens, S. R. Moheimani, *Innovations in piezoelectric shunt damping*, *Smart Structures and Devices*, International Society for Optics and Photonics (2001), pp. 89–102.

[14] A. Fleming, S. Behrens, S. Moheimani, *Reducing the inductance requirements of piezoelectric shunt damping systems*, Smart materials and structures, Vol. 12, No. 1, (2003), p. 57.

[15] A. Cigada, S. Manzoni, M. Redaelli, M. Vanali, *Optimization of the current flowing technique aimed at semi-passive multi-modal vibration reduction*, Journal of Vibration and Control, Vol. 18, No. 2, (2012), pp. 298–312.

[16] N. Van Der Aa, H. Ter Morsche, R. Mattheij, *Computation of eigenvalue and eigenvector derivatives for a general complex-valued eigensystem*, Electronic Journal of Linear Algebra, Vol. 16, No. 1, (2007), p. 26.

[17] G. Habib, G. Kerschen, *Linearization of Nonlinear Resonances Through the Addition of Intentional Nonlinearities*, *Recent Trends in Applied Nonlinear Mechanics and Physics*, Springer (2018), pp. 215–225.

[18] T. Detroux, L. Renson, L. Masset, G. Kerschen, *The harmonic balance method for bifurcation analysis of large-scale nonlinear mechanical systems*, Computer Methods in Applied Mechanics and Engineering, Vol. 296, (2015), pp. 18–38.

[19] O. Thomas, J.-F. Deü, J. Ducarne, *Vibrations of an elastic structure with shunted piezoelectric patches: efficient finite element formulation and electromechanical coupling coefficients*, International journal for numerical methods in engineering, Vol. 80, No. 2, (2009), pp. 235–268.

[20] T. Detroux, G. Habib, L. Masset, G. Kerschen, *Performance, robustness and sensitivity analysis of the nonlinear tuned vibration absorber*, Mechanical Systems and Signal Processing, Vol. 60, (2015), pp. 799–809.